Effect of Process Gas and Powder Quality on Aluminum Alloys Processed by Laser Based Powder Bed Melting Process

D. M. Bauer[a,c†], K. Dietrich[b], M. Walter[a], P. Forêt[b], F. Palm[a], Prof. Dr.-Ing. habil. G. Witt[†]

[a] Airbus Group Innovations – Light alloys, ceramics and processes, Munich, Germany
[b] Linde AG – Linde Gas Division, Unterschleissheim, Germany
[†]University Duisburg – Essen, Institute of Product Engineering, Duisburg, Germany

Abstract

The production of parts and components by Additive Layer Manufacturing (ALM) offers potential cost benefits for aeronautic applications. Laser Based Powder Bed Melting Process offers design flexibility while enabling weight reduction due to topological optimization by substitute conventional design and manufacturing routes. Especially aluminum alloys are highly sensitive to oxygen and hydrogen impurity during the process. Due to this, it is mandatory to control precisely and hold a low oxygen level while processing. Hereby it is possible to avoid any negative impact on the final mechanical properties as tensile strength and fatigue resistance.

For the investigations, aluminum powder (Al-Si-Mg) is used. This paper will present the influence of the oxygen level during processing on the final mechanical properties of the part. Even if pure Argon is commonly used to inert the chamber, different sources of oxygen like powder, equipment and gas supply have a negative impact and will be investigated.[1]–[4]

Introduction

Additive Layer Manufacturing (ALM) offers compared to conventional design and manufacturing routes benefits in cost reduction, design flexibility and the possibility of lead time reduction. An ALM related process is the Laser Based Powder Bed Melting Process (LBM). Aeronautic materials like titanium and aluminum alloys are already established for the LBM process. The serial production of LBM parts for titanium alloys is planned on particular parts within the next years. The uses of aluminum alloys for the LBM process show a high sensitivity and complexity for welding, an affinity to hydrogen porosity and oxidation. Due to this further investigations are substantial.[4], [5]

The build process and quality is mainly influenced by parameters like scanning speed, hatch spacing, laser power and layer thickness. Also the powder quality and process gas are directly influencing the mechanical properties of the produced part. Due to a good weldability and lightweight, aluminum silicon magnesium alloys are commonly used for aeronautic applications. [1], [3], [6]–[8]

The aim of this paper is to investigate the influence of the powder quality and process gas. Current situation show that the majority of the ALM machines run with a higher value than 1000 ppm process gas contamination by oxygen and moisture. For a precisely measurement of oxygen contamination and controlled process atmosphere the existing LBM machine is improved by an external cabinet developed by Linde AG and Airbus Group Innovations. This enables a reliable oxygen measurement as well as active control of the oxygen contamination in the process chamber. Two powders are processed under three different process gas levels for a defined parameter set: > 1000 ppm, 500 ppm and 30 ppm. The chemistry is measured for the raw material (powder) and molten material. To examine the mechanical properties tensile testing are accomplished.

Experimental

I.   Powder characterization

For the investigations two AlSi10Mg powders supplied by two different powder suppliers are examined. In the following the powders are referenced as powder A and B. The atomization method is unknown. Powder delivery requirement for the particle size distribution is between 20 to 63 μm. Further information are investigated in former investigations of D. M. Bauer et al [9].

A scanning electron microscope (Zeiss Auriga FIB-SEM) is used to describe the powder morphology in terms of skin deep shape, satellites appearance, agglomeration rate and surface texture. Shown in Figure 1.
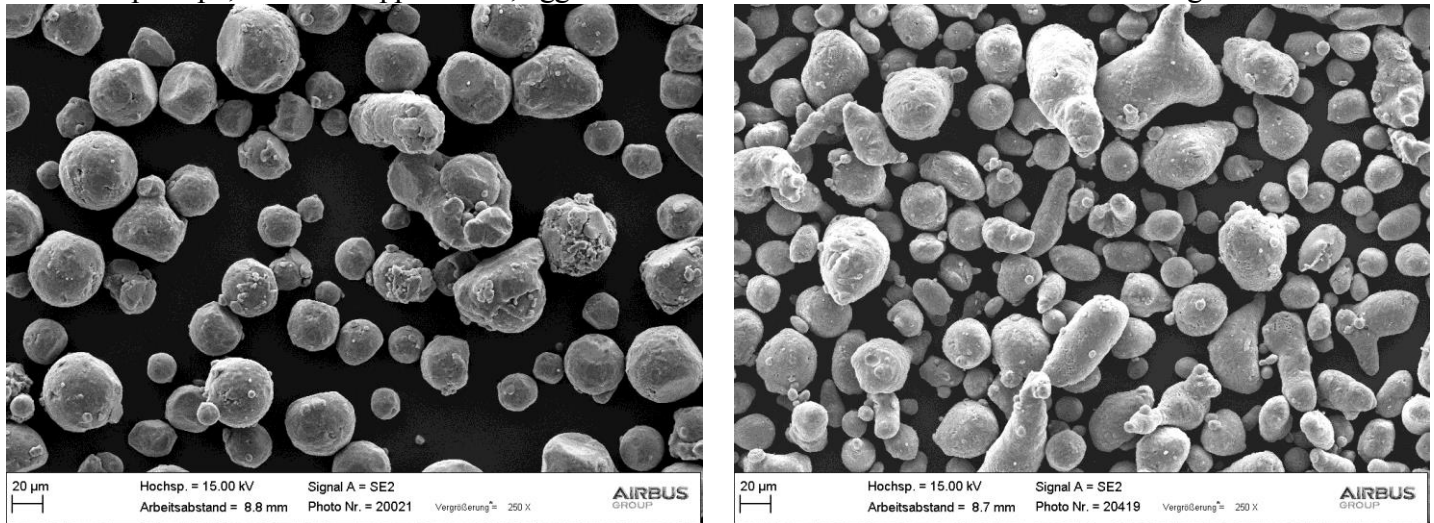

Figure 1: SEM pictures of powder A (left) and powder B (right)

Particle size distribution (PSD) is done with an optical measurement system (Malvern Morphologi G3), which analyzes the particles by a camera. A defined powder volume is dispersed by pressurized air onto a glass plate. The particles are characterized by the commonly used values D10, D50 and D90. Also a sphericity (spherical, non-spherical) measurement is done. The value of rest is not possible to determine. Results of PSD are shown in Table 1.

Table 1: Particle size distribution of powder A and B measured for powder income characterization.

Powder	D10 [μm]	D50 [μm]	D90 [μm]	Spherical [%]	Non Spherical [%]	Rest [%]
A	25	45	65	40	59	1
B	32	53	79	10	87	3

To examine the powder flowability a dynamically measurement system (Revolution Powder Analyser, Mercury Scientific Inc.) is used. A volume of 100 ml powder is filled into a drum between two glass fronts whereon a camera system detects the avalanches due to the rotation of the drum. For each powder five test series of 150 avalanches are measured to calculate an average angle. The results of powder flowability measurement are shown in Table 2.

Table 2: Flowability measurement of powder A and B.

Powder	Average angle	Gradient
A	50	0.053
B	49	0.064

The chemical composition is measured by Inductively Coupled Plasma Optical Emission Spectroscopy (ICP-OES). The Silicon content is determined by gravimetric measurement. The oxygen content (amount of process related powder and molten oxidation) is measured by carrier gas hot extraction. The chemical composition of powder A and B are shown in Table 3.

Table 3: Chemical composition of powder A and B.

Powder	Al [wt%]	Si [wt%]	Mg [wt%]	Mn [wt%]	O [wt%]
A	Rest	9.78	0.31	0.001	0.027
B	Rest	9.88	0.31	0.002	0.095

II.   Gas characterization

Gas supply

Argon is supplied for this investigation with 5.0 quality and is stored in liquid form outside of the building. Welding gases are classifies and designates shielding gases in accordance to DIN EN ISO 14175:2008-06 (Welding consumables – Gases and gas mixtures for fusion welding and allied processes). Rest impurities are nitrogen and carbon dioxide.

Table 4: Impurities in technical gases in accordance to DIN EN ISO 14175:2008-6

Gas quality	Argon [%]	Oxygen [ppm]	H_2O [ppm]
4.6	> 99.996	< 4	< 5
4.8	> 99.998	< 3	< 5
5.0	> 99.9990	< 2	< 3

Gas analysis with Linde Gas Management

Linde Gas and Airbus Group Innovations implemented a gas management system to monitor and regulate the oxygen level in the process chamber of the LBM machine. Therefore a nozzle is installed in the process gas flow. Therewith it is possible to analyze the process gas for oxygen and moisture content. Afterwards it is possible to regulate the oxygen level to a set point. Figure 2 shows the schematic structure of the implemented Linde Gas Management System.
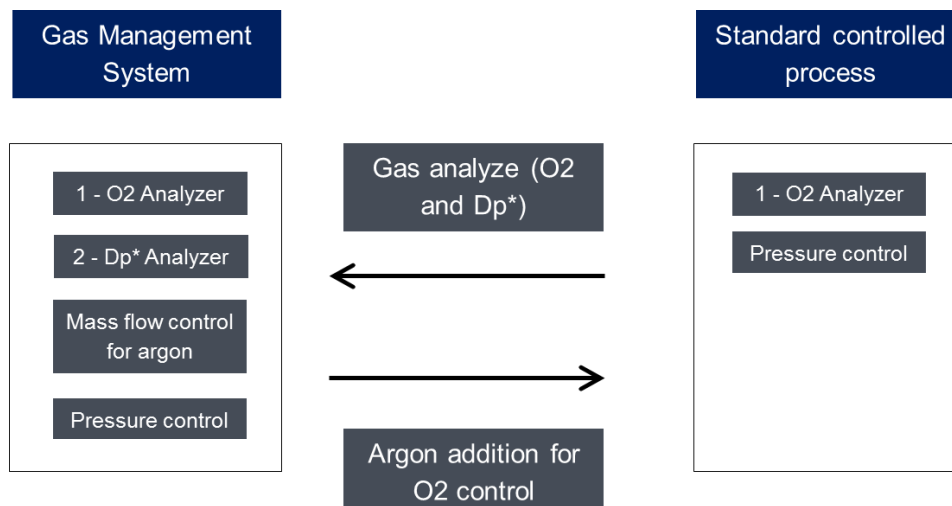

Figure 2: Schematic structure of the Linde Gas Management System. (Dp* = dew point)

Results and discussion

Cross sections

Figure 3 shows the cross section for the standard oxygen controlled atmosphere for powder A. Close under the surface spherically shaped gas pores can be detected. Compared to the standard controlled process, Figure 4 shows the cross section of the 30 ppm controlled oxygen atmosphere. For the higher magnification the lack of fusion is clear to see. No gas pores close to the surface can be investigated. Similar results show Figure 5 (30 ppm oxygen controlled atmosphere) and Figure 6 (standard oxygen controlled atmosphere).
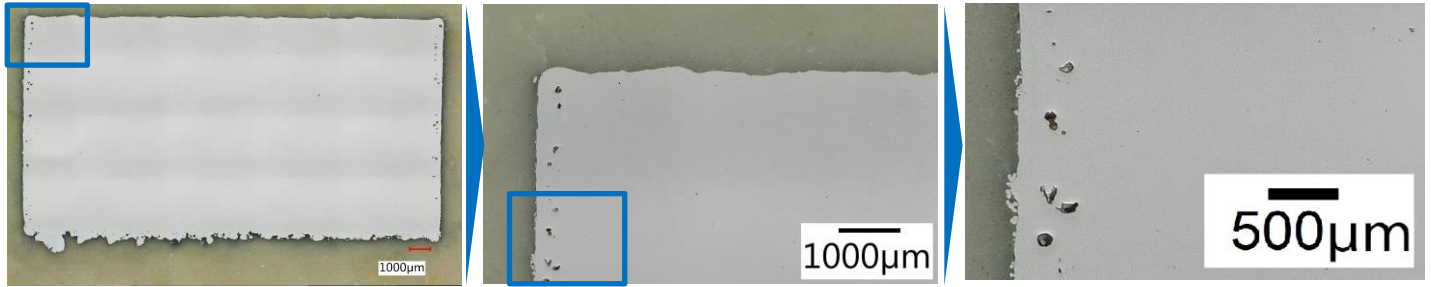
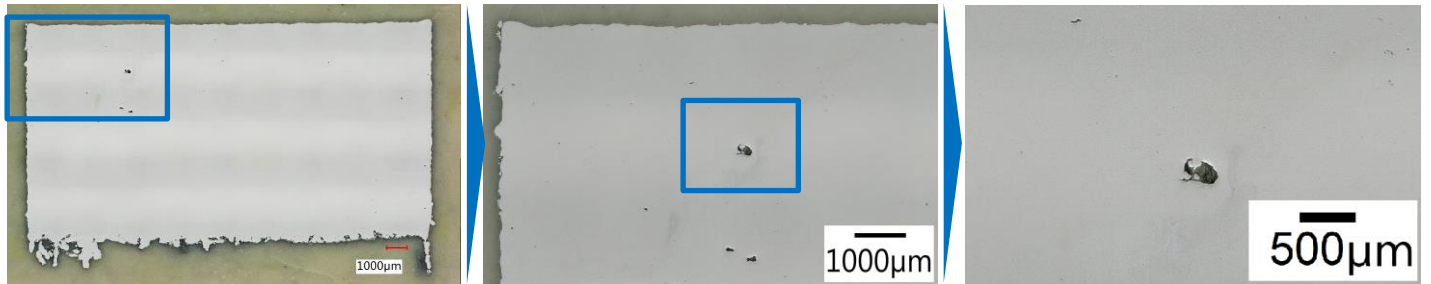**Figure 3: Cross section of density cubes (standard oxygen controlled atmosphere) for powder A**

Figure 4: Cross section of density cubes (30 ppm oxygen controlled atmosphere) for powder A

Figure 5: Cross section of density cubes (standard oxygen controlled atmosphere) for powder B
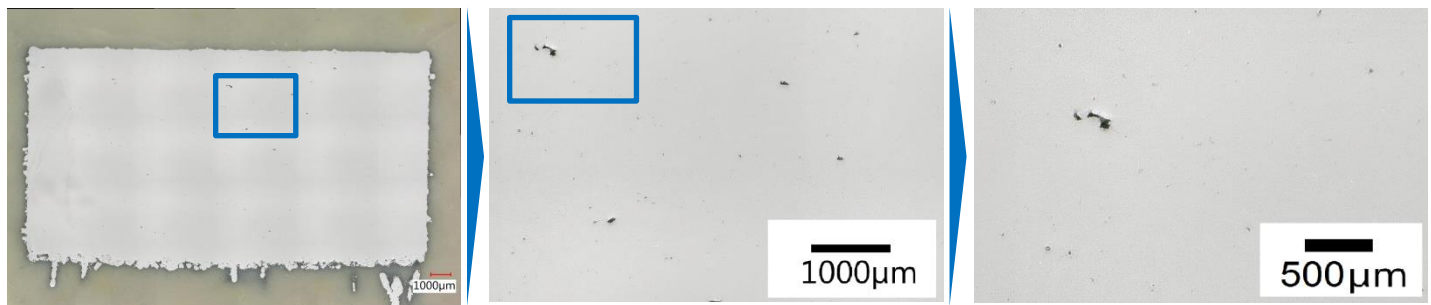

Figure 6: Cross section of density cubes (30 ppm oxygen controlled atmosphere) for powder B

Mechanical properties

The specimens shown in Table 5 are aged for 6 h/ 170 °C and air cooled. For each condition 5 specimens are tested. Build direction is in horizontal direction (XY). The specimens are machined to the final tensile test geometry B4x20 in accordance to DIN 50125. Static tensile tests are performed at ambient condition on a universal testing machine (Zwick 1474 100kN). The amount of Si and Mg are directly influencing achievable maximum strength. As the results show the amount of precipitation hardening possible by the Mg partition which leads to the evolution of coherent Mg2Si particles by the above mentioned post built heat treatment will be an additional strength factor. On to powder material oxide contamination, it seems the oxygen contamination of the build chamber penalizes final material ductility and its plasticity. The results of powder B show for the three different gas contamination lower achievable mechanical properties.

Table 5: Mechanical properties of powder A and B (30 ppm, 500 ppm and uncontrolled oxygen contamination)

Powder	Youngs Modulus [GPa]	Yield Strength [MPa]	UTS [MPa]	A [%]	Z [%]
A-30 ppm O₂	79	335 ± 4.0	471 ± 1.3	6,7 ± 0.9	3,8 ± 0.03
A-500 ppm O₂	78	337 ± 2.4	472 ± 1.0	5,8 ± 1.0	3,8 ± 0.03
A-uncontrolled O₂	78	326 ± 2.0	464 ± 1.6	6,1 ± 0.8	3,8 ± 0.03
B-30 ppm O₂	75	311 ± 3.7	449 ± 1.6	7,0 ± 1.3	3,8 ± 0.02
B-500 ppm O₂	77	293 ± 2.8	437 ± 1.5	7,1 ± 1.3	3,8 ± 0.04
B-uncontrolled O₂	81	291 ± 3.4	439 ± 1.9	6,7 ± 0.9	3,8 ± 0.02

Fracture surface analysis

Figure 7 and Figure 8 show the fracture analysis for tensile specimens, build up in the standard and 30 ppm oxygen controlled atmosphere for powder A. Build direction is z-direction. Figure 7 shows the surface fracture with a fine microstructure. Pores can be seen clear, highlighted by the white circles, as detected for the cross sections, shown in Figure 3. Compared to the standard process the specimens build up in the 30 ppm oxygen controlled atmosphere show less pores as shown in Figure 8. The white highlighted areas show lack of fusion, detected and shown in Figure 4. For both conditions the elongation of around 7 % is confirmed by the honeycomb structure of the fracture.

Powder B shows similar results with the difference of a higher porosity for the specimens build up in the 30 ppm oxygen controlled atmosphere.
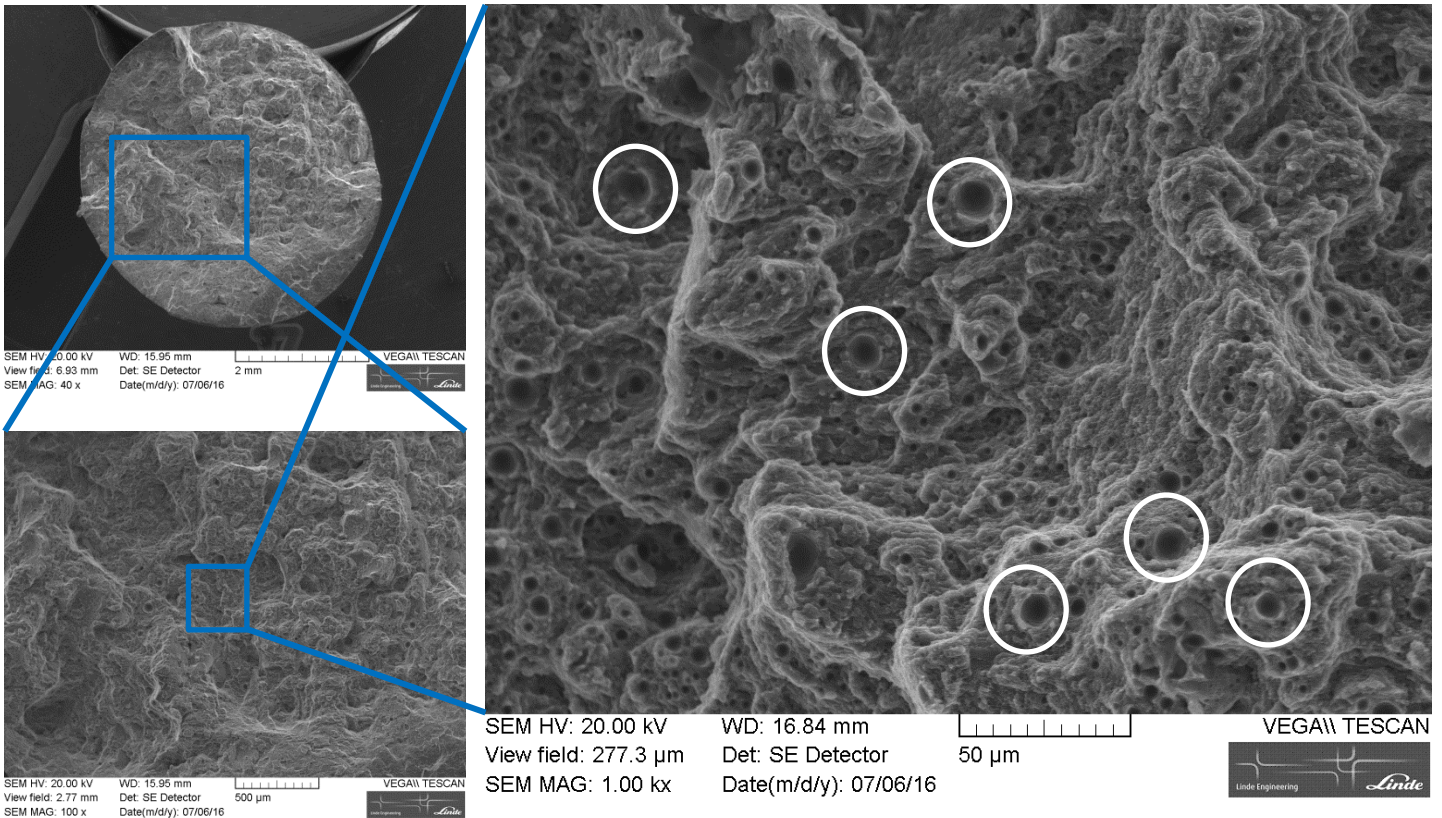
Figure 7: Fracture analysis for tensile specimen build in standard oxygen controlled atmosphere for powder A
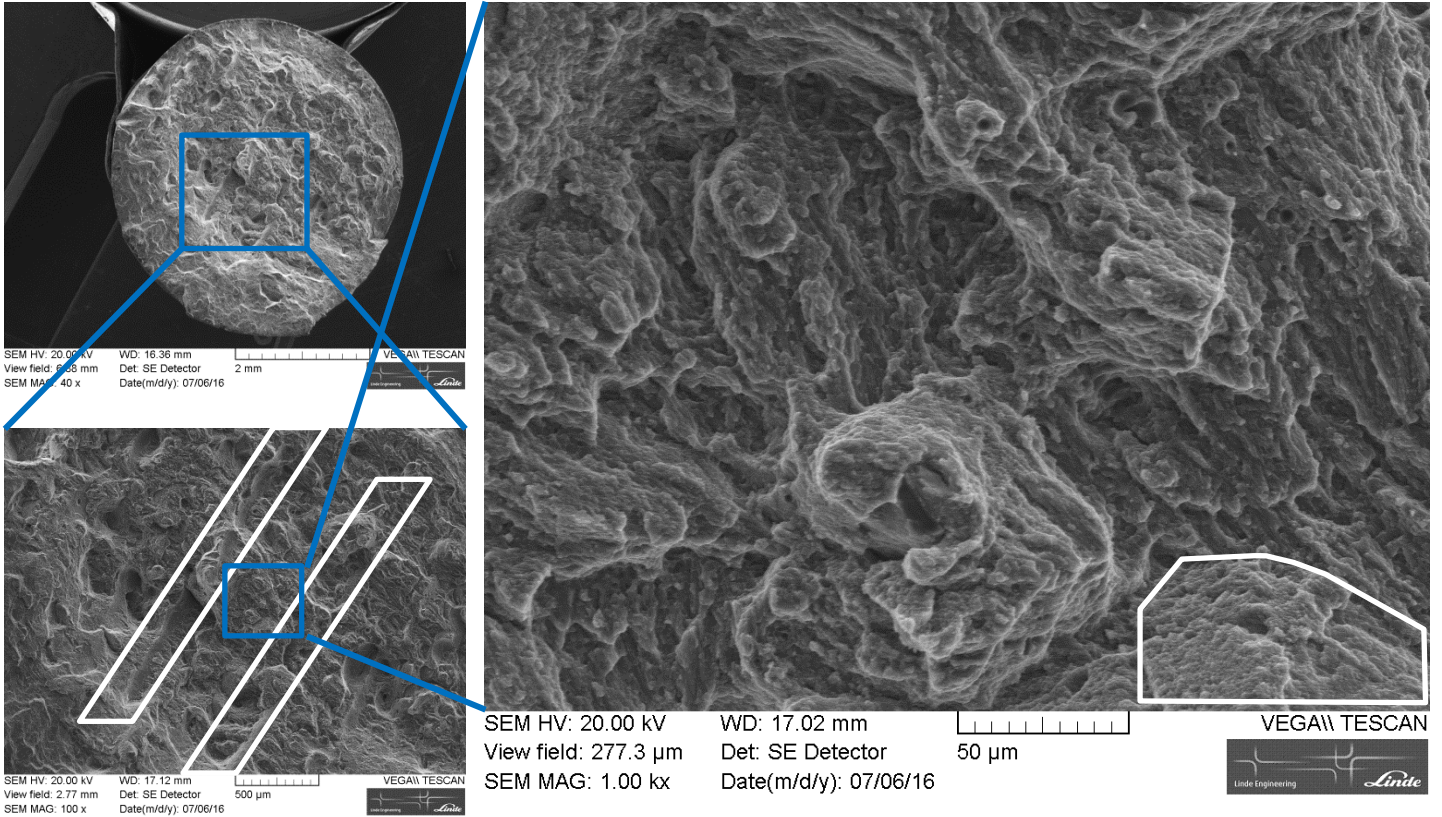

Figure 8: Fracture analysis for tensile specimen build in 30 ppm oxygen controlled atmosphere for powder A

Conclusion

For the investigations AlSi(Mg) alloy powders of two different suppliers with different oxygen contents (270ppm and 950ppm) are used. The samples were processed under three different atmospheres (30ppm, 500ppm and uncontrolled[>1000ppm] of oxygen contamination).
The results of the investigation show:

- Reduction of gas porosity for a controlled process gas atmosphere of 30 ppm. However, consequently, an adjustment of process parameters is mandatory
- Oxide contamination of the build chamber appears to have a direct impact on the chemical composition and thus on the mechanical properties of the final part
- Oxide contamination seems to penalize final material ductility and its plasticity

To process AlSi(Mg) alloys in a reproducible manner, an accurate and precise oxygen monitoring and especially a controlling system are mandatory. Increasing the process reliability for the Laser Based Powder Bed Melting Process is possible by measuring and controlling precisely the oxygen content in the atmosphere and in the powder.

Acknowledgements

Literature

[1]   L. Thijs, K. Kempen, J. P. Kruth, and J. Van Humbeeck, "Fine-structured aluminium products with controllable texture by selective laser melting of pre-alloyed AlSi10Mg powder," *Acta Mater.*, vol. 61, no. 5, pp. 1809–1819, 2013.

[2]   E. Louvis, P. Fox, and C. J. Sutcliffe, "Selective laser melting of aluminium components," *J. Mater. Process. Technol.*, vol. 211, no. 2, pp. 275–284, 2011.

[3]   a. B. Spierings, N. Herres, and G. Levy, "Influence of the particle size distribution on surface quality and mechanical properties in AM steel parts," *Rapid Prototyp. J.*, vol. 17, no. 3, pp. 195–202, 2011.

[4]   K. Kempen, L. Thijs, E. Yasa, M. Badrossamay, W. Verheecke, and J. P. Kruth, "Process optimization and microstructural analysis for selective laser melting of AlSi10Mg," in *22nd Annual International Solid Freeform Fabrication Symposium - An Additive Manufacturing Conference, SFF 2011*, 2011, pp. 484–495.

[5]   C. Weingarten, D. Buchbinder, N. Pirch, W. Meiners, K. Wissenbach, and R. Poprawe, "Formation and reduction of hydrogen porosity during selective laser melting of AlSi10Mg," *J. Mater. Process. Technol.*, vol. 221, pp. 112–120, 2015.

[6]   J.-P. P. Kruth, P. Mercelis, J. Van Vaerenbergh, L. Froyen, M. Rombouts, J. Van Vaerenbergh, L. Froyen, M. Rombouts, J. Van Vaerenbergh, L. Froyen, and M. Rombouts, "Binding mechanisms in selective laser sintering and selective laser melting," *Rapid Prototyp. J.*, vol. 11, no. 1, pp. 26–36, 2005.

[7]   L. N. Carter, C. Martin, P. J. Withers, and M. M. Attallah, "The influence of the laser scan strategy on grain structure and cracking behaviour in SLM powder-bed fabricated nickel superalloy," *J. Alloys Compd.*, vol. 615, pp. 338–347, 2014.

[8]   J.-P. Kruth, B. Vandenbroucke, J. Van Vaerenbergh, and I. Naert, "Rapid Manufacturing of Dental Prostheses by means of Selective Laser Sintering / Melting," *J. Dent. Technol.*, no. 2, pp. 24–32, 2007.

[9]   D. M. Bauer, I. Ludwig, D. Greitemeier, F. Palm, and G. Witt, "Additive manufactured aluminum alloys based on different powder grades," no. March, pp. 1–5, 2016.